The New Nickel Gallium Boride, B14Ga3Ni27: Synthesis and Crystal Structure

Monique Tillard, C. Belin

The New Nickel Gallium Boride, $B_{14}Ga_3Ni_{27}$: Synthesis and Crystal Structure

Monique TILLARD and Claude BELIN*

Agrégats, Interfaces, Matériaux pour l'Énergie, Institut Charles Gerhardt, UMR 5253 CNRS UM2, CC1502, Université de Montpellier 2, Sciences et Techniques du Languedoc, 2 Place Eugène Bataillon, 34095 Montpellier Cedex, France

TITLE RUNNING HEAD: The New Nickel Gallium Boride, $B_{14}Ga_3Ni_{27}$

*CORRESPONDING AUTHOR: Monique TILLARD

Email mtillard@univ-montp2.fr, phone 33 4 67 14 48 97, fax 33 4 67 14 33 04.

ABSTRACT

Crystals of the new compound $B_{14}Ga_3Ni_{27}$ were successfully prepared by arc melting of the elements. $B_{14}Ga_3Ni_{27}$ crystallizes as a novel structure type in the monoclinic space group $P2_1/m$ with unit cell parameters a = 8.6863(8), b = 10.7435(9), c = 8.8431(8) Å, β = 90.670(8) ° and Z = 2. Its structure was solved from single crystal data and refined to $R_1(F) = 0.0465$. The unit cell of $B_{14}Ga_3Ni_{27}$ contains boron dumbbells and isolated gallium atoms embedded in a nickel 3D-framework. Its electronic structure, calculated by DFT methods, indicates metallic properties.

KEYWORDS

Crystal structure, Nickel, Gallium, Boride, DFT calculations, electron density map

INTRODUCTION

It has been recently reported that "Boron displays unusual properties; contrary to other group 13 elements as aluminum and gallium behaving as metals, it has a smaller nucleus holding on to the electrons tighter and behaves more like an insulator". [1,2] The presence of boron has often provided materials with superconducting properties. Elemental boron itself, as well as boron-doped diamond, silicon or silicon carbide, display superconducting transitions at more or less low temperatures. The properties of nickel borocarbides RNi_2B_2C (R = rare earth), discovered in 1994, [3-7] interestingly result from the interplay between superconductivity and magnetism. The simple boride MgB_2 also displays a superconducting transition at T_c = 39 K. [8]

Four binary nickel-rich borides are reported in the phase diagram: NiB, Ni_4B_3, Ni_2B and Ni_3B. [9] There are some ternary compounds containing nickel, boron and another element from group 13: the Pearson crystal database [10] reports about a dozen compounds in the B–M–Ni system (M = Al, Ga or In) where crystal structures have remained not well known. All these compounds having formulae $B_yM_zNi_x$ crystallize in the cubic system with nickel ratio x/(y+z) varying from 1.3 to 3.1. These gallium-containing compounds either belong to the so-called τ-borides $(MM')_{23}B_6$ or are boron-doped derivatives of Ni_3Ga. Compound B_7GaNi_{12}, which stands out from these families, had only unit cell parameters determined, given without any further crystallographic information[11]. Attempts to prepare a compound of composition B_7GaNi_{12} led us to the new ternary gallium nickel boride $B_{14}Ga_3Ni_{27}$, the synthesis and crystal structure determination of which are described below. At the time this manuscript was being written, the syntheses and crystal structures of two novel ternary borides were published:

B_8GaNi_{12} and $B_6Ga_{0.4}Ni_{10.6}$. [12] Although the stoichiometry of the title compound $B_{14}Ga_3Ni_{27}$ is fairly close to that of B_8GaNi_{12}, their crystal structures are quite different.

EXPERIMENTAL SECTION

Synthesis: The elements B (Johnson Matthey, 99%), Ni (Fluka, analysis grade) and Ga (Rhone Poulenc, 6N) were used without further purification. Although the gallium melting point is low (303 K), alloying with Ni and B that melt respectively at 1726 K and 2349 K requires a high temperature, which is difficult to attain in classical furnaces. Boron and nickel powders were intimately mixed and pressed together with gallium into a pellet to be fused in an arc-melting furnace. The main problem in such an experiment is a slight loss of gallium due to its low boiling point relative to B and Ni, and it is necessary to work with an excess of gallium. The ingot was broken several times, finely ground and pressed for arc melting to improve its homogeneity. Nevertheless, the final product, examined under a stereoscopic microscope after coarse crushing, did not appear completely homogeneous.

Crystallographic study: Some well-defined small pieces of the product of the above reaction were selected to be checked for their crystallinity and found to display the required quality for a single crystal X-ray diffraction study. The most regular-shaped and best diffracting crystal was glued to the tip of a glass fiber and mounted on an Xcalibur CCD (Oxford diffraction) four-circle diffractometer using MoK_α radiation for intensity measurements.

The collected data displayed a net trend to centrosymmetry while the extinction conditions were compatible with $P2_1/m$ and $P2_1$ monoclinic space groups. The single crystal structure was solved with program SHELXS97 [13] in the $P2_1/m$ monoclinic cell of parameters a =

8.6863(8), b = 10.7435(9), c = 8.8431(8) Å and β = 90.670(8) °. The structure was then refined using the program SHELXL97. [14] Details of the single crystal data collection and structural refinement are given in Table 1. The 26053 recorded reflections (including symmetry equivalent and redundant ones) within the complete diffraction sphere (θ from 2.98 to 32.98 °) displayed no evidence for a centered lattice; they were merged into 3250 unique reflections. The direct methods of SHELXS indicated the presence of nine light and 19 heavier electron densities in the Fourier map. Hence, in a first step, the structure was refined with 19 nickel and nine boron atoms. This led to obviously too small atomic displacement parameters for three nickel sites whose positions were then assigned to gallium. Once the crystal composition was known, the data were corrected for absorption effects (μ = 34.73 mm^{-1}) using the analytical numerical procedure included in the CrysAlis software. [15]

The final refinement was carried out using anisotropic atomic displacement parameters for Ga, Ni and isotropic displacement parameters for B atoms. It yielded $R_1(F)$ = 0.0465 and $wR_2(F^2)$ = 0.0886 (2334 independent reflections with $I > 2\sigma(I)$ and 181 refined parameters). The atomic positional and displacement parameters are given in Table 2 and some selected interatomic distances are presented in Table 3.

To consider the possibility of solid solutions and the occurrence of atomic mixing in such a structure, all site occupation factors were checked. The use of free variables for their refinement showed that gallium and nickel sites do not deviate far from full site occupation. Freely refined independently, occupations of 2e and 4f sites filled with nickel converged in the ranges 0.499(3)-0.502(3) and 0.999(5)-1.007(5), respectively. The occupations of 2e sites assigned to gallium refined to 0.494(3)-0.501(3) when filled with gallium and to 0.554(3)-0.563(3) when filled with nickel. However Ga/Ni mixing was tested on these sites and, within 2sigma limits, refinements indicated full occupation of these sites with gallium. Note that R1 values and ADP were not affected by such modifications. The site occupation factors also

converged to full occupation for boron atoms, therefore the final refined composition is $B_{14}Ga_3Ni_{27}$.

EDX analysis: Some single crystals, previously identified by X-ray diffraction and displaying the monoclinic structure, were analyzed using a Oxford Instrument Environmental Scanning Electron Microscope. This device, equipped with a X-Max large area SDD sensor, allows excellent sensitivity/precision/resolution, including for the analysis of light elements (all elements from Be to Pu can be analyzed). These crystals were found to contain B, Ga and Ni in proportions very close to that determined by XRD (B/Ga/Ni ratio was 4.8(5)/1.03(4)/9).

CALCULATION METHOD

Calculations were performed at the DFT level with the code CASTEP [16, 17] using the gradient-corrected GGA-PW91 exchange and correlation functional. [18] CASTEP uses plane-wave basis sets to treat valence electrons and pseudo potentials to approximate the potential field of ion cores. Ultra-soft pseudo potentials (USPP) generated for each element according to the Vanderbilt [19] scheme were chosen. Boron was considered with three valence electrons while, for Ni and Ga, the inner 3*d* levels were added as valence states. Kinetic cut-off energies were set at fine qualities (300 eV) and Monkhorst-Pack uniform grids of automatically generated k-points were used. [20] Accurate cell parameter and atomic position optimizations were carried out within monoclinic symmetry, and unit cell parameters did not deviate from the experimental by more than 0.7%.

STRUCTURAL DESCRIPTION, RESULTS AND DISCUSSION

The crystal structure of the new compound $B_{14}Ga_3Ni_{27}$ is represented in figure 1. The nickel atoms are found at general 4f and special 2e positions and form a complex three-dimensional network in which are embedded boron dumbbells and "isolated" gallium atoms. Among the three independent gallium atoms located at 2e special positions, atom Ga1 is surrounded, at distances ranging from 2.425(2) to 2.795(2) Å, by 12 Ni atoms forming a distorted cuboctahedron. On the other hand, atom Ga2 with 12 Ni neighbors at distances comprised between 2.512(2) and 2.851(2) Å, and atom Ga3 with 11 Ni neighbors (from 2.517(2) to 2.798(2) Å) display less symmetrical environments. It is interesting to note that gallium atoms have no close contact with boron, a situation already observed in $B_6Ga_{0.4}Ni_{10.6}$. [10]

In the $B_{14}Ga_3Ni_{27}$ structure, boron atoms occur as B_2 dumbbells distributed over the unit cell within four layers perpendicular to the b-axis (figure 2). In the layer centered at y = 0, the boron dimers are tilted approximately parallel to the direction [0 1 1] instead of [0 1 $\bar{1}$] in the layer at y = ½. The two remaining layers (y = ¼ and y = ¾) not only contain boron dimers parallel to the (0 1 0) plane but also all the gallium atoms of the structure. The interatomic distances in the boron dumbbells vary from 1.72(1) to 1.95(2) Å. These values are to be compared with bond lengths reported in the literature: 1.67 Å and 1.75 Å for B_2F_4 and B_2Cl_4.[21, 22] In the three-dimensional network of CaB_4, [23] each dumbbell (B-B = 1.67 Å) is coordinated to four B_6 octahedra while in the high-pressure orthorhombic form of boron, B_2 units (B-B = 1.73 Å) are linked to B_{12} icosahedra. [2, 24] Boron also forms linear trimers (B-B = 1.84 Å) in monoclinic Ni_4B_3, infinite zigzag chains (B-B = 1.88 Å) in orthorhombic Ni_4B_3 and infinite linear chains (B-B = 2.12 Å) in Ni_2B. In the ternary boride $B_8Ga_3Ni_{12}$, isolated B atoms are found together with B_5 oligomeric units as fragments of zigzag chains (B-B ranging from 1.73 to 1.86 Å) while isolated B atoms coexist with infinite zigzag chains (B-B = 1.792

and 1.766 Å) in $B_6Ga_{0.4}Ni_{10.6}$. [10] All these B-B distances are longer than the Pauling single bond length of 1.60 Å. Noteworthy is the double-bonded boron (B-B distance of 1.40 Å) observed within an infinite linear chain in compound LiB. [25]

In $B_8Ga_3Ni_{12}$ recently reported as being isostructural with its aluminum analogue, and in $B_6Ga_{0.4}Ni_{10.6}$, the boron atoms sit inside nickel trigonal prisms three-fold capped by B, Ga or Ni. Instead, in the τ-borides, examples of which are known for the ternary system B-Ga-Ni, boron is present as isolated atoms displaying square anti-prismatic coordination.

In the present compound $B_{14}Ga_3Ni_{27}$, each boron atom is surrounded only by nickel. The coordination polyhedra around atoms B1, B3, B4, B6 and B8 are more or less regular square antiprisms (Ni-B varying from 2.06 to 2.27 Å). These antiprisms, which are fused by square face sharing, form 12-atom coordination polyhedra around B1-B3 or B8-B8 dumbbells (figure 3). In the case of the B7-B9 dumbbell, Ni atoms lying around B7 (2.05 to 2.73 Å) and B9 (2.04 to 2.31 Å) are arranged within an 11-atom coordination polyhedron. The Ni atoms around B5 and B2, distances to which range respectively from 2.02 to 2.13 Å and 2.06 to 2.21 Å, form 7-atom polyhedra which condense by square face sharing with the adjacent antiprisms filled with B6 and B4 into 11-atom coordination polyhedra centered by B5-B6 or B2-B4 dumbbells (figure 3).

On the other hand, all the Ni atoms have short-range contacts to 3, 4 or 5 boron atoms and Ni-B distances varying from 2.02 to 2.27 Å are in the range usually found for other nickel borides (2.03 to 2.29 Å in Ni_3B for example).

The calculated CASTEP band structure indicates a metallic character for $B_{14}Ni_{27}Ga_3$. However no band crosses the Fermi level at YA and EC segments[1] of the irreducible Brillouin zone. This would predict some anisotropy in the electrical conduction (figure 4). The main contributions in the total DOS at Fermi level involve the 2p B, 4p Ga and 3d Ni levels. The

[1] Y (0 ½ 0) A (-½ ½ 0) E(-½ ½ ½) C(0 ½ ½)

overlap populations calculated for B-B bonds of 1.72 to 1.94 Å range from 0.82 to 0.50, this underlines the localized covalent character of the structure at boron dumbbells. The populations calculated for B-Ni pairs ranging from 0.20 to 0.45 are also indicative of some bonding interactions between these atoms. Overlap values obtained for Ni-Ni and Ni-Ga pairs are very small. Atomic Mulliken charges are -0.6 for boron, 1.6 to 2 for gallium and range from 0.02 to 0.20 for nickel, in fairly good agreement with Pauling's electronegativities (2.0, 1.6 and 1.8 respectively). Keeping in mind that Mulliken charge and population analyses are known to be basis set dependent and therefore of limited use when calculated with plane-wave DFT methods, it seems better to analyze these results using electron density plotting. The deformation charge density, computed by subtracting densities of the isolated atoms from the total electron density, is particularly interesting because it shows positive regions indicative of bond formation while negative regions point out electron losses (figure 5). It is evident that the highest bonding electron population lies at B-B and to a less extent at Ni-B atomic pairs. The metallic character of the structure is then featured by the absence of localized electron density between Ni and Ga as well as between Ni atoms.

CONCLUSION

The structural determination of $B_{14}Ga_3Ni_{27}$ brings a new example of a transition metal boride which takes place in the family of nickel borides between cubic τ-borides and orthorhombic compounds B_8GaNi_{12} and $B_6Ga_{0.4}Ni_{10.6}$. With an M/B ratio of 3.83, the τ-borides are characterized by the presence of isolated boron atoms surrounded by Ni antiprisms.

The compounds B_8GaNi_{12} and $B_6Ga_{0.4}Ni_{10.6}$ (M/B ratio of 1.65 and 1.83) also contain isolated B atoms besides B_5 oligomers or infinite zigzag chains. In these two compounds,

three-fold capped trigonal prisms of Ni surround boron atoms. Interestingly, boron occurs as dimers in the compound $B_{14}Ga_3Ni_{27}$, which has an intermediate M/B ratio of 2.14. The boron atoms are located at centers of the coordination polyhedra whose geometries vary from the 8-atom antiprism to 7-atom less regular polyhedra; the latter could be seen as a step towards the trigonal prismatic geometry.

In all these compounds, the formation of B-B bonds within dimers, oligomers or polymers is associated with the fusion, by face sharing, of Ni polyhedra. In $B_{14}Ga_3Ni_{27}$, as well as in $B_6Ga_{0.4}Ni_{10.6}$, the gallium atoms are found without any direct contact with boron, whereas only one or two long-range contacts are to be considered in B_8GaNi_{12}. This might be the sign of a weak affinity between the elements B and Ga within intermetallic compounds and more particularly, it explains the paucity of Ga-B binary compounds in contrast with Al-B.

$B_{14}Ga_3Ni_{27}$ is expected to display metallic properties as indicated by the DFT calculations that show a quite delocalized electron density over the whole structure beside the rather high electron density localized between boron atoms featuring some covalence.

Acknowledgements

The authors are grateful to D. Granier for data collection measurements on the CCD Oxford diffractometer.

REFERENCES

(1) Research news of Stony Brook University, 9, **2009**, http://www.stonybrook.edu/research/news/RN/resnew090210.html.

(2) Oganov, A. R.; Chen, J.; Gatti, C.; Ma, Y.; Ma, Y.; Glass, C. W.; Liu, Z.; Yu, T.; Kurakevych, O. O.; Solozhenko, V. L., *Nature* **2009,** *457*, 863-867.

(3) Cho, B.K.; Canfield, P.C.; Miller, L.L.; Johnston, D.C.; Beyermann, W. P.; Yatskar, A., *Phys. Rev. B* **1995,** *52*, 3684.

(4) Eisaki, H.; Takagi, H.; Cava, R. J.; Batlogg, B.; Krajewski, J. J.; Peck, W. F.; Jr., K. M.; Lee, J. O.; Uchida, S., *Phys. Rev. B* **1994,** *50*, 647.

(5) Lynn, J.W.; Skanthakumar, S.; Huang, Q.; Sinha, S.K.; Hossain, Z.; Gupta, L.C.; Nagarajan, R.; Godart, C. *Phys. Rev. B* **1997**, *55*, 6584.

(6) Cava, R. J.; Takagi, H.; Zandbergen, H. W.; Krajewski, J. J.; Peck Jr., W. F.; Siegrist, T.; Batlogg, B.; van Dover, R. B.; Felder, R. J.; Mizuhashi, K.; Lee, J. O.; Eisaki, H.; Uchida, S., *Nature (London)* **1994,** *367,* 252.

(7) Shinha, S. K.; Lynn, J. W.; Grigereit, T. E.; Hossain, Z.; Gupta, L. C.; Nagarajan, R.; Godart, C., *Phys. Rev. B* **1995,** *51*, 681.

(8) Nagamatsu, J.; Nagakawa, N.; Muranaka, T.; Zenitani, Y.; Akimitsu, J., *Nature* **2001,** *410*, 63.

(9) Schobel, J. D.; Stadelmaier, H. H., *Z. Metallkd.* **1965,** *56(12)*, 856.

(10) Villars, P.; Cenzual, K., *Pearson's Crystal Data: crystal structure database for inorganic compounds, release* **2009/10**, ASM international, Material Park, Ohio, USA.

(11) Chaban, N.F.; Kuz'ma,Y.B. Dopov. Akad. Nauk. Ukr. RSR (ser. A), **1973**, 550.

(12) Ade, M.; Kotzott, D.; Hillebrecht, H., *Journal of Solid State Chemistry* **2010,** *183 (8)*, 1790-1797.

(13) Sheldrick, G. M., **1997**, *SHELXS 97: A Program for Crystal Structures Solution.* University of Göttingen. Germany.

(14) Sheldrick, G. M., **1997**, *SHELXL97: A Program for Refining Crystal Structures*. University of Göttingen. Germany.

(15) *CrysAlis'Red' 171 software package*, **2004,** Oxford diffraction Ltd, Abingdon, United Kingdom.

(16) Kresse, G.; Forthmuller, J., *J. Comput. Mater. Sci.* **1996,** *6*, 15.

(17) Kresse, G.; Forthmuller, J., *Phys. Rev.B* **1996,** *54*, 11169.

(18) Perdew, J. P.; Chevary, J. A.; Vosko, S. H.; Pederson, M. R.; Singh, D. J.; Fiolhais, C., *Phys. Rev. B* **1992,** *46*, 6671.
(19) Vanderbilt, D., *Phys. Rev. B* **1990,** *41*, 7892-7895.
(20) Monkhorst, H. J.; Pack, J. D., *Phys. Rev. B* **1997,** *16*, 1748.
(21) Atoji, M.; Wheatley, P. J.; Lipscomb, W. N., *J. Chem. Phys.* **1957,** *27*, 196-199.
(22) Trefonas, L. M.; Lipscomb, W. N., *J. Chem. Phys.* **1958,** *28*, 54-55.
(23) Schmitt, R.; Blaschkowski, B.; Eichele, K.; Meyer, H. J., *Inorg. Chem.* **2006,** *45*, 3067-3073.
(24) Zarechnaya, E. Y.; Dubrovinsky, L.; Dubrovinskaia, N.; Miyajima, N.; Filinchuk, Y.; Chernyshov, D.; Dmitriev, V., *Sci. Technol. Adv. Mater.* **2008,** *9*, 044209.
(25) Liu, Z.; Qu, X.; Huang, B.; Li, Z., *J. Alloys Compds* **2000,** *311*, 256.

FIGURE AND TABLE CAPTIONS

Figure 1. Representation of the atom distribution in the monoclinic unit cell of $B_{14}Ga_3Ni_{27}$, approximately viewed along the b-axis. Four cells have been represented to emphasize the packing of B dumbbells (orange) and Ga atoms (blue) in the Ni three-dimensional network (green). Ga atoms are drawn inside their nearest neighbor Ni polyhedra.

Figure 2. Representation of the monoclinic structure of $B_{14}Ga_3Ni_{27}$ approximately viewed along the a-axis showing the ordered distribution of boron dumbbells: B_2 units in layers around y = 0, ½ and B_2 units plus Ga atoms in layers around y = ¼, ¾.

Figure 3. Nickel coordination around boron dumbbells: fused square antiprisms (12-atom polyhedron) around B1-B3 and B8-B8 and the different geometries for the 11-atom polyhedra around B5-B6, B7-B9 and B2-B4 (if the long distance of 2.56Å is omitted).

Figure 4. CASTEP band structure and densities of states (total and partial DOS) calculated for $B_{14}Ga_3Ni_{27}$. No band crosses the Fermi level at YA and EC segments predicting some anisotropy in the electrical conduction. Densities of states at Fermi level mainly involve boron 2p and nickel 3d contributions.

Figure 5. The electron density difference calculated with CASTEP for $B_{14}Ga_3Ni_{27}$. High densities, indicative of bond formation, are encountered mainly between boron atoms and to a less extent between boron and nickel while density is diffuse within Ni-Ni and Ni-Ga atomic pairs.

Table 1. Crystal data and structure refinement for $B_{14}Ga_3Ni_{27}$

Table 2. Atomic coordinates (x 10^4) and equivalent isotropic displacement parameters (Å^2 x 10^3) for $B_{14}Ga_3Ni_{27}$. U_{eq} is defined as one third of the trace of orthogonalized U_{ij} tensor.

Table 3. Selected bond lengths [Å] in $B_{14}Ga_3Ni_{27}$ (boron dumbbells and shortest interatomic distances).

Supplementary material

Table S1. Anisotropic displacement parameters (Å^{2}x 10^3) for $B_{14}Ga_3Ni_{27}$. The anisotropic displacement factor exponent takes the form: $-2\pi^2[h^2a^{*2}U_{11} + ... + 2\ h\ k\ a^*\ b^*\ U_{12}]$.

Table 1. Crystal data and structure refinement for $B_{14}Ga_3Ni_{27}$

Crystal system	Monoclinic
Space group	$P2_1/m$, 11
Lattice constants	
a (Å)	8.6863(8)
b (Å)	10.7435(9)
c (Å)	8.8431(8)
β (°)	90.670(8)
Volume ($Å^3$)	825.19(13)
Formula	$B_{14}Ga_3Ni_{27}$
Z	2
Formula weight	1945.67
Density (Mg/m^3)	7.831
F(000)	1838
Crystal shape and color	dark grey triangular fragment
Crystal size (mm)	0.089 x 0.064 x 0.040
Absorption coefficient (mm^{-1})	34.727
Max/min transmission factors	0.38, 0.14
θ range (°)	2.98 - 32.98
Reflections collected	26053
Independent reflections	3250 [R(int) = 0.0826]
Observed reflections [$I > 2\sigma(I)$]	2334
Refinement method	Full-matrix least squares on F^2
Parameters / restraints	181 / 0
Extinction coefficient	0.00034(8)
Goodness-of-fit on F^2	0.956
Final R indices [$I > 2\sigma(I)$]	$R_1(F) = 0.0465$, $wR_2(F^2) = 0.0886$
R indices (all data)	$R_1(F) = 0.0967$, $wR_2(F^2) = 0.1091$
Weighting scheme	$w = 1/[\sigma^2(F_o^2) + (0.0501P)^2]$, $P = (F_o^2 + 2F_c^2)/3$
Largest diff. peak and hole ($e.Å^{-3}$)	1.635 and -1.508

Table 2. Atomic coordinates (x 10^4) and equivalent isotropic displacement parameters ($Å^2$ x 10^3) for $B_{14}Ga_3Ni_{27}$. U_{eq} is defined as one third of the trace of orthogonalized U_{ij} tensor.

	Position	x	y	z	U_{eq}
Ga(1)	2e	2774(2)	2500	6701(2)	8(1)
Ga(2)	2e	8591(2)	2500	8365(2)	10(1)
Ga(3)	2e	1060(2)	2500	2460(2)	10(1)
Ni(1)	2e	3724(2)	2500	3692(2)	8(1)
Ni(2)	2e	7915(2)	2500	1741(2)	6(1)
Ni(3)	2e	5690(2)	2500	7579(2)	7(1)
Ni(4)	2e	-272(2)	2500	5706(2)	8(1)
Ni(5)	4f	2053(2)	2500	9773(2)	9(1)
Ni(6)	4f	3873(1)	1147(1)	1281(1)	8(1)
Ni(7)	4f	1738(1)	998(1)	4835(1)	8(1)
Ni(8)	4f	9635(1)	1073(1)	381(1)	8(1)
Ni(9)	4f	7369(1)	1207(1)	5805(1)	8(1)
Ni(10)	4f	913(1)	1073(1)	7763(1)	7(1)
Ni(11)	4f	9112(1)	1007(1)	3511(1)	7(1)
Ni(12)	4f	4571(1)	934(1)	5703(1)	7(1)
Ni(13)	4f	6553(1)	1167(1)	9819(1)	8(1)
Ni(14)	4f	1613(1)	53(1)	2151(1)	9(1)
Ni(15)	4f	3846(1)	853(1)	8498(1)	7(1)
Ni(16)	4f	6075(1)	1187(1)	3129(1)	8(1)
B(1)	2e	5775(16)	2500	5007(15)	9(2)
B(2)	2e	5553(16)	2500	1440(15)	9(3)
B(3)	2e	7707(17)	2500	4107(16)	11(3)
B(4)	2e	4556(15)	2500	9645(14)	5(2)
B(5)	4f	7822(11)	519(9)	1684(11)	9(2)
B(6)	4f	1881(11)	508(9)	9903(11)	9(2)
B(7)	4f	6016(11)	598(9)	7659(10)	8(2)
B(8)	4f	368(11)	-525(9)	4183(10)	7(2)
B(9)	4f	3665(11)	581(9)	3608(10)	6(2)

Table 3. Selected bond lengths [Å] in $B_{14}Ga_3Ni_{27}$ (boron dumbbells and shortest interatomic distances).

B(1)-B(3)	1.87(2)
B(2)-B(4)^{ii}	1.799(18)
B(5)-B(6)^{i}	1.806(13)
B(7)-B(9)^{i}	1.715(13)
B(8)-B(8)^{iii}	1.947(19)
B(5)-Ni(11)	2.024(10)
Ga(1)-Ni(10)	2.4245(16)
Ni(9)-Ni(14)^{i}	2.4172(15)
B(1)-Ga(1)	3.022(14)

Symmetry transformations used to generate equivalent atoms
^{i} -x+1,-y,-z+1, ^{ii} x,y,z-1, ^{iii} -x,-y,-z+1

Table S1. Anisotropic displacement parameters ($Å^2$x 10^3) for $B_{14}Ga_3Ni_{27}$.The anisotropic displacement factor exponent takes the form: $-2\pi^2[h^2a^{*2}U_{11} + ... + 2 h k a^* b^* U_{12}]$

	U_{11}	U_{22}	U_{33}	U_{23}	U_{13}	U_{12}
Ga(1)	8(1)	7(1)	10(1)	0	0(1)	0
Ga(2)	8(1)	9(1)	12(1)	0	1(1)	0
Ga(3)	10(1)	10(1)	11(1)	0	0(1)	0
Ni(1)	9(1)	5(1)	9(1)	0	0(1)	0
Ni(2)	7(1)	5(1)	7(1)	0	0(1)	0
Ni(3)	9(1)	4(1)	8(1)	0	1(1)	0
Ni(4)	8(1)	6(1)	9(1)	0	-1(1)	0
Ni(5)	9(1)	7(1)	10(1)	0	0(1)	0
Ni(6)	8(1)	9(1)	7(1)	1(1)	0(1)	-3(1)
Ni(7)	5(1)	9(1)	9(1)	-2(1)	1(1)	-1(1)
Ni(8)	7(1)	9(1)	8(1)	0(1)	1(1)	0(1)
Ni(9)	7(1)	8(1)	9(1)	2(1)	2(1)	2(1)
Ni(10)	7(1)	7(1)	7(1)	0(1)	0(1)	-1(1)
Ni(11)	8(1)	7(1)	6(1)	-1(1)	-1(1)	2(1)
Ni(12)	7(1)	8(1)	7(1)	-1(1)	0(1)	-1(1)
Ni(13)	9(1)	8(1)	7(1)	0(1)	-2(1)	1(1)
Ni(14)	7(1)	13(1)	6(1)	2(1)	0(1)	-1(1)
Ni(15)	7(1)	7(1)	7(1)	0(1)	1(1)	-1(1)
Ni(16)	8(1)	8(1)	7(1)	1(1)	1(1)	-1(1)

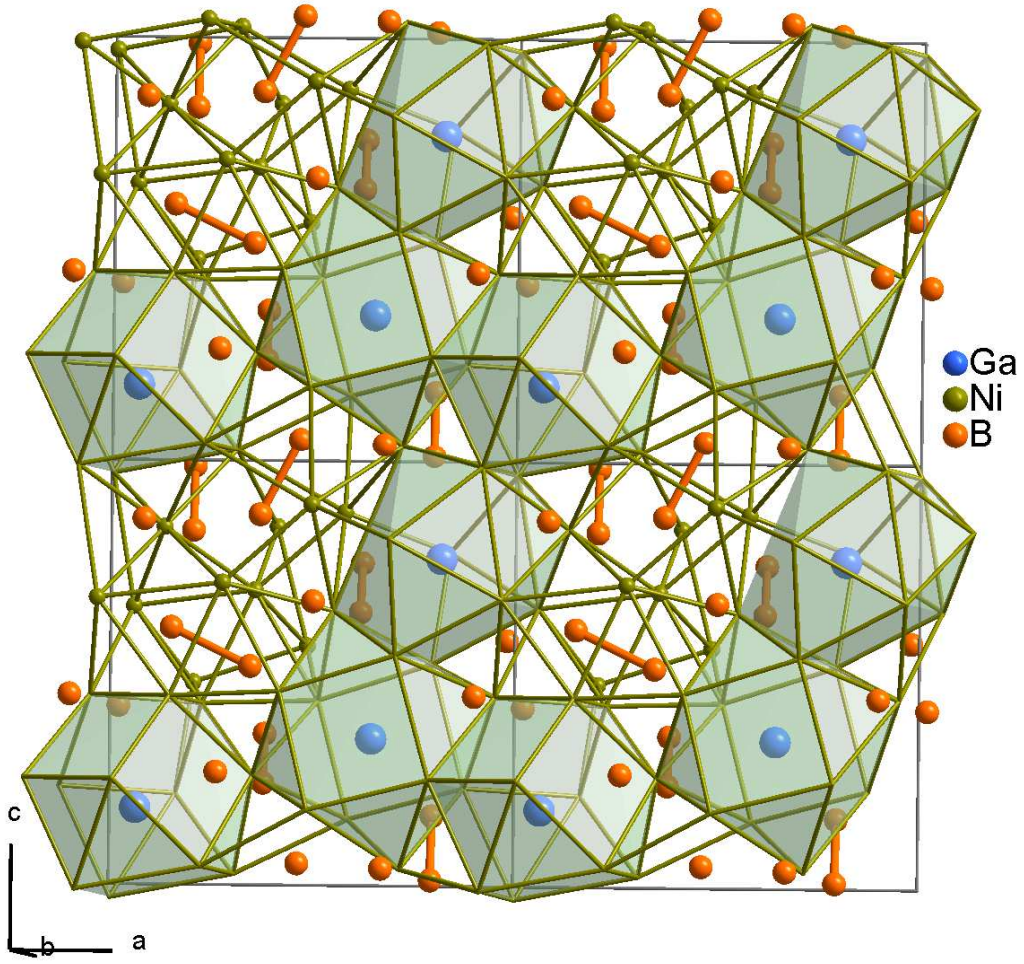

Figure 1. Representation of the atom distribution in the monoclinic unit cell of $B_{14}Ga_3Ni_{27}$, approximately viewed along the b-axis. Four cells have been represented to emphasize the packing of B dumbbells (orange) and Ga atoms (blue) in the Ni three-dimensional network (green). Ga atoms are drawn inside their nearest neighbor Ni polyhedra.

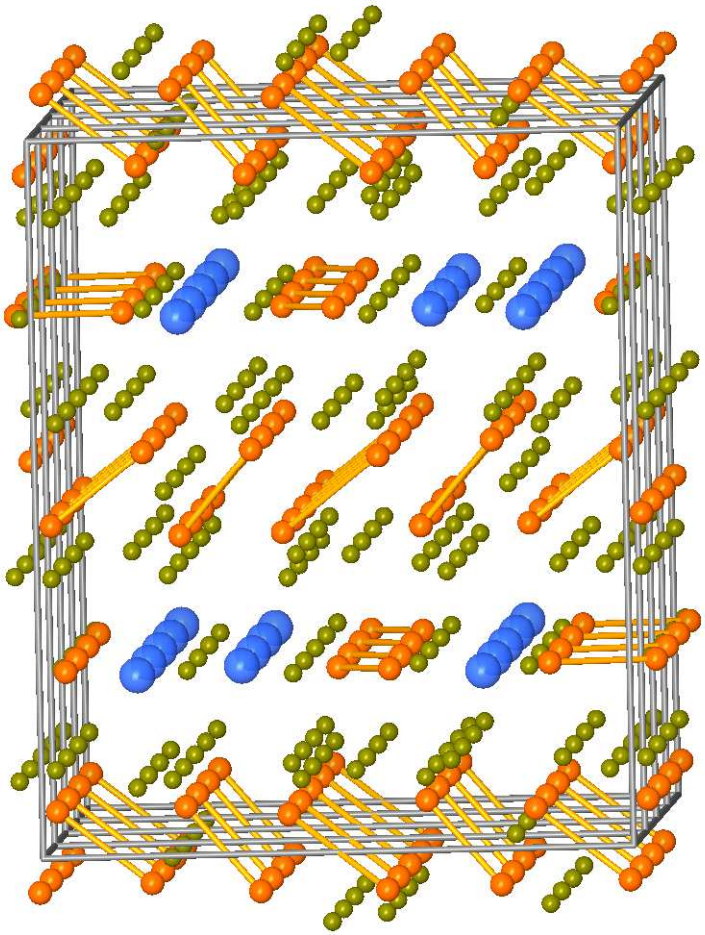

Figure 2. Representation of the monoclinic structure of $B_{14}Ga_3Ni_{27}$ approximately viewed along the a-axis showing the ordered distribution of boron dumbbells: B_2 units in layers around y = 0, ½ and B_2 units plus Ga atoms in layers around y = ¼, ¾

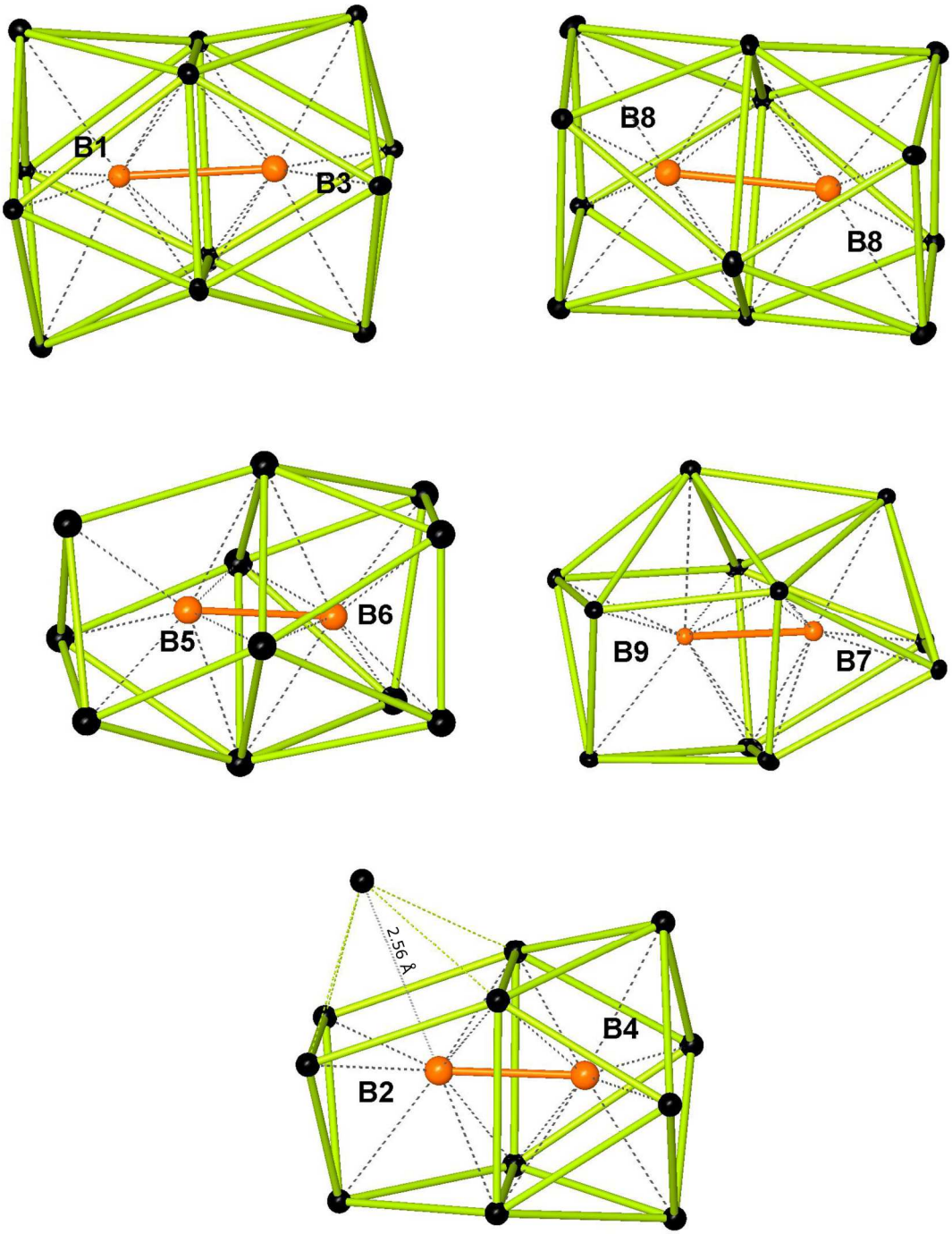

Figure 3. Nickel coordination around boron dumbbells: fused square antiprisms (12-atom polyhedron) around B1-B3 and B8-B8 and the different geometries for the 11-atom polyhedra around B5-B6, B7-B9 and B2-B4 (if the long distance of 2.56Å is omitted).

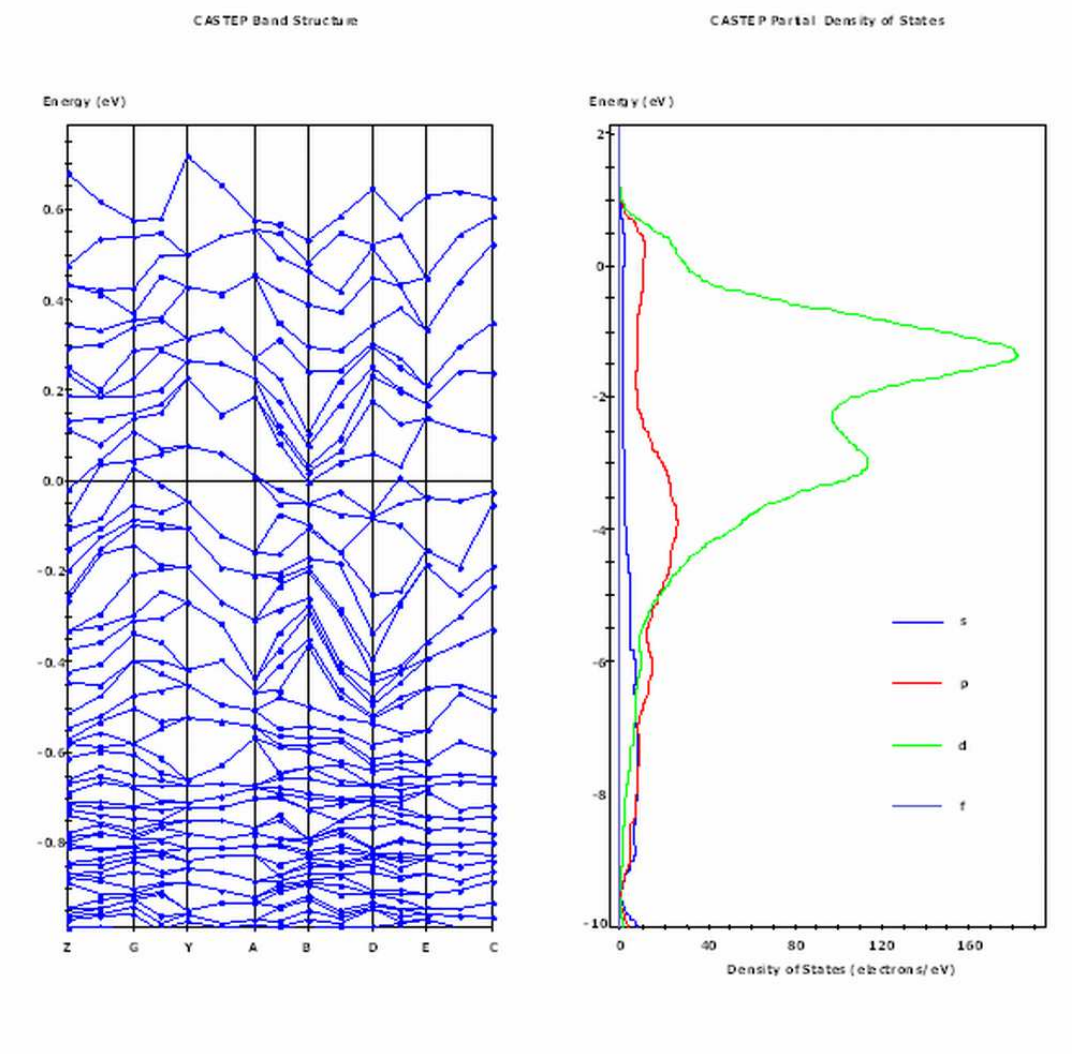

Figure 4. CASTEP band structure and densities of states (total and partial DOS) calculated for $B_{14}Ga_3Ni_{27}$. No band crosses the Fermi level at YA and EC segments predicting some anisotropy in the electrical conduction. Densities of states at Fermi level mainly involve boron 2p and nickel 3d contributions.

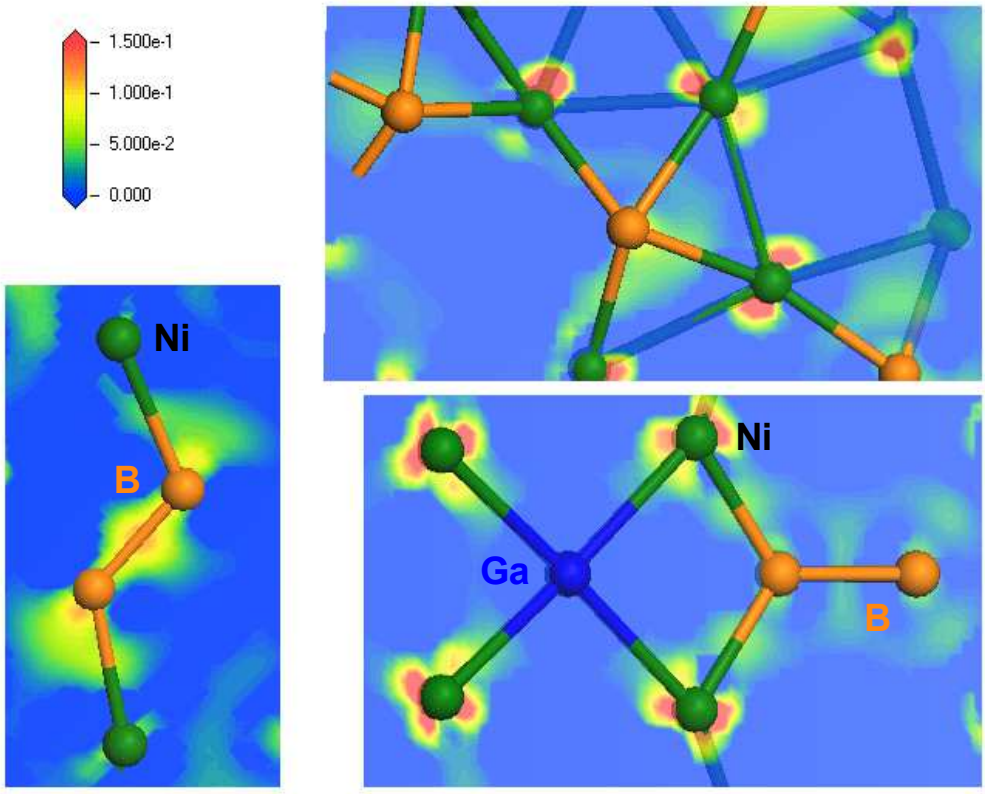

Figure 5. The electron density difference calculated with CASTEP for $B_{14}Ga_3Ni_{27}$. High densities, indicative of bond formation, are encountered mainly between boron atoms and to a less extent between boron and nickel while density is diffuse within Ni-Ni and Ni-Ga atomic pairs.

SYNOPSIS TOC

$B_{14}Ga_3Ni_{27}$ crystallizes as a novel structure type in the monoclinic space group $P2_1/m$ with unit cell parameters a = 8.6863(8), b = 10.7435(9), c = 8.8431(8) Å, β = 90.670(8) °. The structure of $B_{14}Ga_3Ni_{27}$ contains boron dumbbells and isolated gallium atoms embedded in a nickel 3D-framework and its electronic structure indicates metallic properties.

SYNOPSIS GRAPHIC

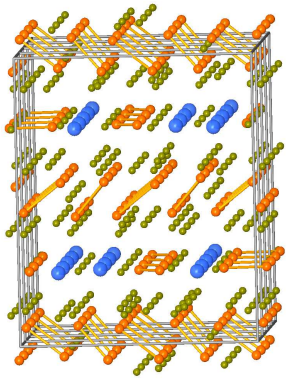

1. *Research news of Stony Brook University, 9, (2009), http://www.stonybrook.edu/research/news/RN/resnew090210.html.*
2. Oganov, A. R.; Chen, J.; Gatti, C.; Ma, Y.; Ma, Y.; Glass, C. W.; Liu, Z.; Yu, T.; Kurakevych, O. O.; Solozhenko, V. L., *Nature* **2009,** *457* (7231), 863-867.
3. B.K. Cho; P.C. Canfield; L.L. Miller; D.C. Johnston; Beyermann, W. P.; Yatskar, A., *Phys. Rev. B* **1995,** *52*, 3684.
4. Eisaki, H.; Takagi, H.; Cava, R. J.; Batlogg, B.; Krajewski, J. J.; Peck, W. F.; Jr., K. M.; Lee, J. O.; Uchida, S., *Phys. Rev. B* **1994,** *50*, 647.
5. J.W. Lynn; S. Skanthakumar; Q. Huang; S.K. Sinha; Z. Hossain; L.C. Gupta; Nagarajan, R.; Godart, C., *Phys. Rev. B* **1997,** *55*, 6584.
6. R.J. Cava; H. Takagi; H.W. Zandbergen; J.J. Krajewski; W.F. Peck Jr.; T. Siegrist; B. Batlogg; R.B. van Dover; R.J. Felder; K. Mizuhashi; J.O. Lee; Eisaki, H.; Uchida, S., *Nature (London)* **1994,** *367* 252.
7. Shinha, S. K.; Lynn, J. W.; Grigereit, T. E.; Hossain, Z.; Gupta, L. C.; Nagarajan, R.; Godart, C., *Phys. Rev. B* **1995,** *51*, 681.
8. Nagamatsu, J.; Nagakawa, N.; Muranaka, T.; Zenitani, Y.; Akimitsu, J., *Nature* **2001,** *410*, 63.

9. Schobel, J. D.; Stadelmaier, H. H., *Z. Metallkd.* **1965,** *56(12)*, 856.
10. Villars, P.; Cenzual, K., *Pearson's Crystal Data : crystal structure database for inorganic compounds release 2009/10, ASM international, Material Park, Ohio, USA.*
11. Chaban, N. F.; Kuz'ma, Y. B., *Dopov. Akad. Nauk Ukr. RSR (Ser. A)* **1973**, 550.
12. Ade, M.; Kotzott, D.; Hillebrecht, H., *Journal of Solid State Chemistry* **2010,** *183* (8), 1790-1797.
13. Oganov, A. R.; Chen, J.; Gatti, C.; Ma, Y.; Ma, Y.; Glass, C. W.; Liu, Z.; Yu, T.; Kurakevych, O. O.; Solozhenko, V. L., *Nature* **2009,** *457*, 863-867